Biomed Eng Lett (2014) 4:201-212
DOI 10.1007/s13534-014-0155-x

REVIEW ARTICLE

The Potential of Naturally Occurring Lasing for Biological and Chemical Sensors

Seung Ho Choi and Young L. Kim

Received: 27 July 2014 / Revised: 15 September 2014 / Accepted: 23 September 2014

Abstract
Although recent advances in biosensing are promising, there still is a need for label-free, sensitive, and cost-effective detection of single nanoparticles and single biomolecules, without relying in complex fabrications and sophisticated detection strategies. In this review, we show that a better understanding of light-matter interactions can lead to the development of advanced biosensing and bioanalysis systems. In particular, we address alternative biosensing methods of taking advantage of naturally occurring lasers (also known as random lasers). In random lasers, resonances are self-formed due to multiple scattering, leading to light amplification and coherent light generation in the presence of amplifying media. In this case, lasing emission can be unprecedentedly sensitive to subtle nanoscale perturbations. Specifically, we discuss the possibility that random lasers can be an alternative yet superior physical mechanism for biosensors, because the random laser biosensing platform is simple and the detection strategy is straightforward. We further envision that random laser biosensors have the potential to facilitate developing enhanced biological and chemical sensors for single-molecule and single-nanoparticle quantitation.

Keywords Biosensors, Disordered photonics, Random lasers, Photoluminescence

Seung Ho Choi, Young L. Kim (✉)
Weldon School of Biomedical Engineering, Purdue University, Indiana 47907, USA
Tel : +1-765-496-2445 / Fax : +1-765-496-1459
E-mail : youngkim@purdue.edu

Young L. Kim
Department of Biomedical Engineering, Kyung Hee University, Yongin 446-701, South Korea

INTRODUCTION

Detections of single molecules and single nanoparticles have attracted a significant amount of interest and research over the past years. To better understand fundamental biological processes (e.g. molecular transport [1, 2], protein folding kinetics [3], and aspects of DNA replication [4]), researchers across a wide range of disciplines have conducted single-nanoparticle detection studies experimentally and numerically. Single-molecule detections has also begun to be applied in clinical research for example in detecting viruses in blood [5], and PBS solution [6]. Traditionally, early work on single-nanoparticle/molecule detection experiments was based on labeling of interest molecules [7, 8]. Specifically, fluorescence labels in fluorescence microscopy, surface enhanced Raman spectroscopy, and confocal microscopy were extensively used to quantify signals from single molecules. However, they relied on prior information on the target's molecules [9] and the molecules were treated chemically to react with the label according to the molecule information [10-14]. To overcome the need of labeling, several attempts have been demonstrated. Such examples include surface plasmon resonance [15-19], reflectometric interference spectroscopy [20], dual polarization interferometer [21], photonic crystal biosensor [22], distributed feedback laser biosensor [23], fiber-optic waveguides [14], nanoparticle probes [24] to nanowires [25], mechanical cantilevers [26], and biochips [27].

Advances in biosensors and bioassays heavily rely on identifications and applications of new physical concepts and phenomena. Among numerous physical mechanisms for biosensing, optical microcavity sensors have recently received considerable attention, because they allow for an unprecedented level of sensitive and accurate detection of target agents at single-nanoparticle or single-molecule levels. In particular, passive microcavities using whispering gallery modes have

been the object of intensive investigation due to high quality factors and sensitive resonant wavelength shifts [28-30]. By using mode splitting in a microcavity, the sizes of individual nanoparticles can also be measured [31]. Recent research has also shown that combining second harmonic light generation with whispering gallery modes can provide an alternative mechanism for detecting nanoscale perturbations [32].

On the other hand, such new biosensors often require complex nanoscale precision fabrications and sophisticated detection strategies. Even the recent advances in fabrications at the nanoscale and microscale levels, allowing constructing defect-free periodic photonic structures. However, there are some limitations to fully eliminate variations and imperfections that might degrade their performance [33-36]. Furthermore, such complex and imperfect fabrication techniques could potentially hamper widespread utilization and translation of optical biosensors. Fortunately, recent approaches in quantum information technology shows that deliberate utilization of irregular disordered photonics structures may provide a way to overcome the limitation of fabrication defects and to serve as efficient photonic structures [37].

In this respect, one approach for the biosensor development is to use an intriguing new physical light confinement phenomenon as known as random lasing, which relies on disordered photonic structures. In contrast to conventional lasers, resonant cavities in random lasers are self-generated by a group of individual scatterers in disordered structures [38-40], whereas conventional lasers require a well-defined optical resonant cavity. Random lasers have being studied in the field of optical physics intensively. This field has been searching for meaningful applications to demonstrate the usefulness of random lasers. The physically new concept and the utilization disordered structures, this alternative detection mechanism over conventional biosensor methods can be used to assess minute alterations at single-molecule or single-nanoparticle levels, as illustrated in Fig. 1.

In this review, we show the potential that random lasing can serve as a novel yet superior biosensing mechanism possessing the following key characteristics: i) Random lasing is sensitive to perturbations in single-nanoparticle levels. ii) Random lasing has multiple emission peaks and those are stable and reproducible. iii) Random lasing can require low lasing threshold. iv) Random lasing can be implemented in a biosensing scheme. v) Random lasers can have simple microstructures that could potentially minimize fabrication defect and variation. First, we briefly present the basic physical principles of random lasing and numerical models. Second, we discuss the key characteristics in details. Finally, we conclude this review to build a foundation for new applications of random lasers as biosensors.

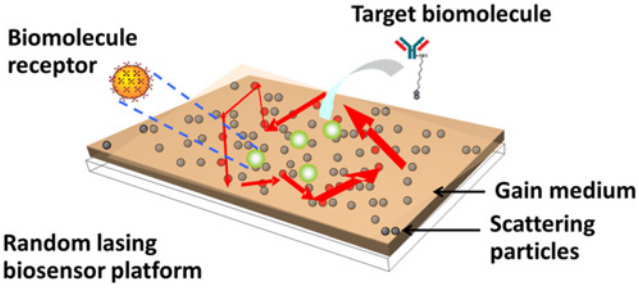

Fig. 1. Conceptual schematic of random lasing biosensors.When a target molecule is attached to a receptor, this subtle alteration in the photonic structures results in changes in the resonant modes, which can be quantified in the emission spectrum or intensity.

PHYSICAL PRINCIPLES OF RANDOM LASING

Introduction of random lasers and sensing mechanism

Conventional lasers consist of an optical gain material and an optical cavity for the system to laser, which determine the mode of a laser (i.e. directionality and frequency), as illustrated in Fig. 2a. On the other hand, in random lasers,

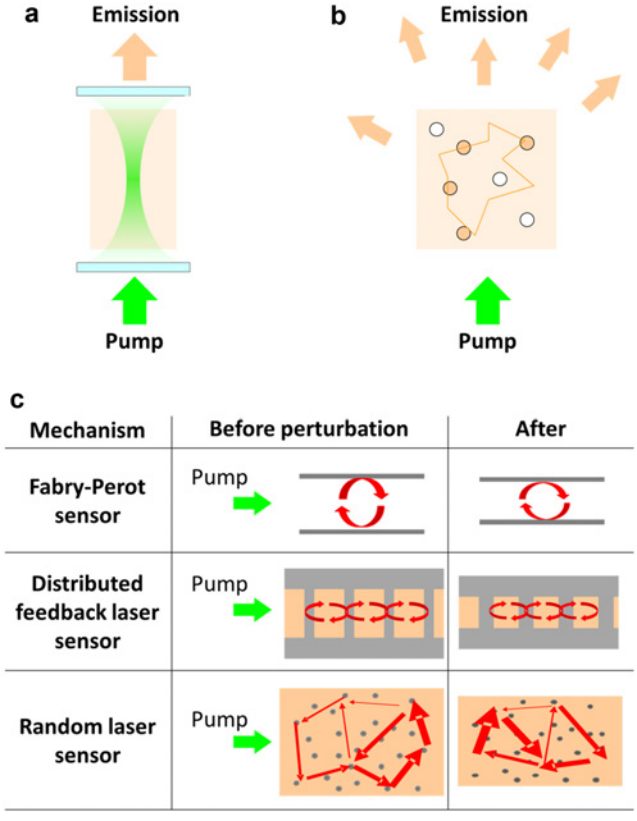

Fig. 2. Comparison between conventional lasers and naturally occurring lasers (i.e. random lasers).(a) A well-configured optical cavity is formed in reflecting mirror in a conventional laser. (b) In a random laser, multiple resonances are self-formed due to multiple scattering. (c) Schematics of three laser sensor mechanisms and potential sensitivities to applied perturbations.

resonant cavities are randomly self-formed due to multiple scattering (Fig. 2b) [38, 40, 41]. This possible existence of the random lasing action is also supported by the enhanced backscattering phenomena [40, 42-44]. Fig. 2c further summarizes similarities and differences of three different laser biosensing mechanisms. Traditionally, Fabry-Perot cavities have been commonly used as a basic sensing mechanism. We can easily understand the basic working principles illustrated in Fig. 2c based on Fabry-Perot optical pressure sensors [45, 46]. In this case, an external perturbation simply changes the cavity configuration, resulting in changes in the lasing emission. As biological and chemical sensing mechanisms, distributed feedback (DFB) sensors (also known as Bragg grating sensors) have been actively used [47]. Since an external perturbation can change the Bragg grating structure, the lasing frequency and emission intensity can be sensitive to alterations resulting from molecule binding and refractive index changes. In general, significant changes in the Bragg grating or the Fabry-Perot cavities are necessary to induce significant alteration in the lasing emission. For example, DFB fiber pressure sensors are intended to reliably sense high pressure values and thus they do not exhibit the same high performance in the low-pressure regime [48, 49]. In this respect, a key feature of random laser sensors is that an extremely small level of applied perturbations can potentially change self-formed multiple resonant modes.

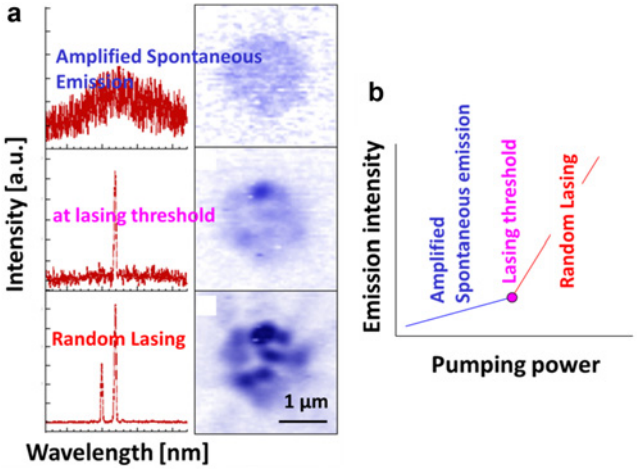

Fig. 3. Emission evolution from spontaneous emission (i.e. fluorescence), amplified spontaneous emission (ASE), to stimulated emission (i.e. lasing). (a) Spectrum and corresponding image for a single particle random laser. This figure is reproduced with permission from Ref [38]. (b) Emission intensity changes as a function of the pump energy or power with lasing threshold behavior.

Amplified spontaneous emission random lasing and coherent random lasing

Random lasing is classified into two fundamental mechanisms: i) Amplified spontaneous emission (ASE) random lasers: In ASE random laser, light amplification is generated from long light path. Interestingly, even internal structure is static, resulting optical cavity or spontaneous emission shows chaotic behavior [50, 51]. Stochastic spikes in the emission spectrum are commonly observed, because they are attributed to spontaneous emission events that are significantly amplified through the long lightpaths. Thus, noise-like emission spikes in ASE random lasers can randomly vary from pulse to pulse. ii) Coherent random lasers: In coherent random laser, resonant cavities are self-generated by a group of individual scatterers in a disordered structure and the each discrete narrow emission peak represents individual lasing mode [52-54]. As shown in Fig. 3, when the pumping power exceeds a lasing threshold, the spontaneous emission changes to coherent random lasing, discrete narrow peaks in spectrum [38]. One fundamental difference between coherent random lasers and ASE random lasers is the emission spectral stability. In coherent random lasers, the spectral properties of the emission are stable and reproducible, because the emission spectrum is determined by the structure and configuration of the medium. If the structure is fixed or static, the location of the multiple emission peaks remains unchanged, as each emission peak corresponds to the definitive laser cavity. Indeed, this is the main characteristic of coherent random lasers that we can exploit as a novel biosensing mechanism.

Random lasers towards biological and chemical sensing

ASE random lasers have shown interesting potential applications, such as temperature sensing [55] and explosive detection [56, 57], after theoretical study [58] and experimental study [59] of ASE random lasing. In respect to coherent random lasers, the origin of discrete random lasing emission peaks was theoretically [60] and experimentally [9, 61-63] studied in several materials such as i) strongly and weakly scattering media [43, 54, 64, 65], ii) nanowires [66] and iii) coreshell nanoparticles [67]. In addition, both ASE and coherent random lasing were also applied in biological tissue and cells: ASE in animal tissue [68, 69], coherent random laser in human colon cancerous tissue [70], coherent random lasers in bovine bone tissue [71], and live cells fused with green fluorescent protein [72]. All of the studies were based on the idea that the lasing emission is highly sensitive to subtle alterations in the photonic structures.

Numerical methods describing random lasing effects

In numerical studies of lasing modes in a 1-dimenional (1D) structure, the transfer matrix method (TMM) is used to solve the Maxwell's equations [73-76]. In a 1D geometry, the Maxwell's equations can mathematically be simplified through

TMM and thus the field components (i.e. E and H) can be expressed as follows [76]:

$$\begin{bmatrix} E_1 \\ H_1 \end{bmatrix} = \prod_{k=2}^{N-1} M_k \begin{bmatrix} E_{N-1} \\ H_{N-1} \end{bmatrix}$$
$$M_k = \begin{bmatrix} \cos k_0 h & (i \sin k_0 h)/Y_1 \\ (i \sin k_0 h) Y_1 & \cos k_0 h \end{bmatrix}, \quad (1)$$
$$Y_1 = \sqrt{\varepsilon_0 / \mu_0}\, n_1 / \cos\theta_k, h = 2 n_1 d_k \cos\theta_k / 2$$

where n ($=\sqrt{\varepsilon}$) is the refractive index, d_k is the thickness of k-th layer, and θ_k is the incidence angle of k-th layer. The dielectric constant of gain contains the negative part which denotes the homogeneous amplification of field [74]. However, in a 1D structure, the introduction of gain does not change the shape of the wave function. The gain just increases the amplitude of wave function uniformly. TMM above is simple but useful to numerically study several 1D random lasing structures.

To numerically investigate 2-dimenional (2D) resonant modes, the time dependent-theory finite difference time domain method (FDTD) is used to solve the Maxwell's equations with the rate equation for an active medium [77, 78]:

$$\frac{dN_3(\vec{r},t)}{dt} = P_r(t) N_0(\vec{r},t) - \frac{N_3(\vec{r},t)}{\tau_{32}}$$
$$\frac{dN_2(\vec{r},t)}{dt} = \frac{dN_2(\vec{r},t)}{\tau_{32}} + \frac{\vec{E}(\vec{r},t)}{\hbar \varpi_a} \cdot \frac{d\vec{P}(\vec{r},t)}{dt} - \frac{N_2(\vec{r},t)}{\tau_{21}}$$
$$\frac{dN_1(\vec{r},t)}{dt} = \frac{dN_2(\vec{r},t)}{\tau_{21}} - \frac{\vec{E}(\vec{r},t)}{\hbar \varpi_a} \cdot \frac{d\vec{P}(\vec{r},t)}{dt} - \frac{N_1(\vec{r},t)}{\tau_{10}}, \quad (2)$$
$$\frac{dN_0(\vec{r},t)}{dt} = \frac{N_1(\vec{r},t)}{\tau_{10}} - P_r(t) N_0(\vec{r},t)$$

where the N_j (j = 0, 1, 2, 3) are the population of atom in four levels, τ_{ij} is the electron transition coefficient from level i to level j, $P_r(t)$ is the external pumping rate, and $\vec{P}(\vec{r}, t)$ is the polarization density as follow:

$$\frac{d^2\vec{P}(\vec{r},t)}{dt^2} + \Delta\varpi_a \frac{d\vec{P}(\vec{r},t)}{dt} + \varpi_a^2 \vec{P}(\vec{r},t) =$$
$$\frac{\Gamma_r}{\Gamma_r} \frac{e^2}{m} [N_1(\vec{r},t) - N_2(\vec{r},t)] \vec{E}(\vec{r},t), \quad (3)$$
$$\Gamma_r = \frac{1}{\tau_{21}}, \Gamma_r = \frac{e^2 \varpi_a^2}{6\pi\varepsilon_0 m c^3}$$

where w_a is the center frequency and Δw_a is the line width of the atomic transition from level 2 to level 1, e is the electron charge and m is its mass. Finally, $\vec{P}(\vec{r}, t)$ is introduced in following well-known Maxwell equation:

$$\nabla \times \vec{E}(\vec{r},t) = -\frac{\partial \vec{B}(\vec{r},t)}{\partial t}$$
$$\nabla \times \vec{H}(\vec{r},t) = \varepsilon(\vec{r}) \frac{\partial \vec{E}(\vec{r},t)}{\partial t} + \frac{\partial \vec{P}(\vec{r},t)}{\partial t}, \quad (4)$$

where $\varepsilon(\vec{r})$ is the dielectric constant of media. In a random lasing study, random particles are described by the spatial fluctuation of the dielectric constant. In the 2D case, the electromagnetic field components above can be decoupled into TM and TE polarizations. In most of random lasing numerical studies [61, 71, 77, 79, 80], E_z, H_x, and H_y, components of the TM mode are usually preferred because of its low lasing threshold [81].

However, FDTD takes significant computational time to access lasing modes. Since, the information about the eigenstates of disordered media and the frequency profile of gain can also be used to accurately predict actual lasing modes [77], another promising approach is to use a finite element method (FEM) [82, 83] to solve the Helmholtz equation for quasimodes, which are identical to lasing modes obtained using the Maxwell's equations with the rate equation. In the Helmholtz equation, vector field components (i.e. $\vec{E}$ and $\vec{B}$) are converted to a single scalar field component (i.e. $V(\vec{r}) = E_z$) and give the following wave equation:

$$\nabla^2 V(\vec{r}) + k^2 n^2(\vec{r}) V(\vec{r}) = 0, \quad (5)$$

where k is the wavevector and n is the refractive index of media. In a further FEM procedure, the above governing equation (Eq. (5)) is discretized and changes to linear simultaneous equations in order to acquire a numerical solution. The solution wavevector is a complex number: $\kappa = \mathrm{Re}(\kappa) + \mathrm{i} \times \mathrm{Im}(\kappa)$, which contains both resonant frequencies and losses. In particular, in a strongly scattering medium, quasimodes can be identical to lasing modes [78, 84, 85]. In this regard, FEM is an appropriate choice for mode studies, because FEM can directly access individual modes of the passive system consisting of a large number of nanoparticles ($<\lambda$) and intrinsically contain less numerical error. Overall, as numerical experiments using TMM, FEM, and FDTD are limited to 1D or 2D structures, pseudo spectral time-domain methods may further be employed for numerical lasing experiments in 3-dimenional (3D) random media [86].

KEY CHARACTERISTICS FOR RANDOM LASING BIOSENSORS

Stable and reproducible emission

Spectral stability is fundamental difference between coherent random lasers and ASE random lasers. In ASE random lasers, stochastic spikes in the emission spectrum are commonly

observed, because they are attributed to spontaneous emission events that are significantly amplified through long light paths [50, 51]. Thus, the noise-like emission spikes in the ASE random lasers randomly change from pulse to pulse. However, when a coherent random laser's pumping intensity exceeds a threshold, the spectral spacing of the adjacent narrow peaks becomes relatively regular. A recent study has also demonstrated that spatially localized and extended random lasing modes can be formed together [87], supporting the spectral stability in coherent random lasers. These studies therefore support the use of coherent random lasers as a biosensing signal due to their proven spectral stability.

In the coherent random laser regime the spectral properties of the emission are reproducible, because the emission spectrum is determined by the structure and configuration of the sample [64, 88, 89]. Indeed, this is the main characteristic of the coherent random lasers for biosensors. If the structure is fixed or static, the location of the multiple emission peaks remains unchanged, because each emission peak corresponds to the definitive laser cavity [64, 88, 89]. Almost all of the studies on coherent random lasers showed that the frequency positions of individual peaks are highly reproducible, when the internal structures or configurations are static or fixed [51, 84, 88-90]. Even in aqueous media, the lasing frequencies were shown to remain the same [84, 85]. Collectively, the emission patterns of coherent random lasers are closely correlated with the structural properties of media such as refractive index and internal structure variations.

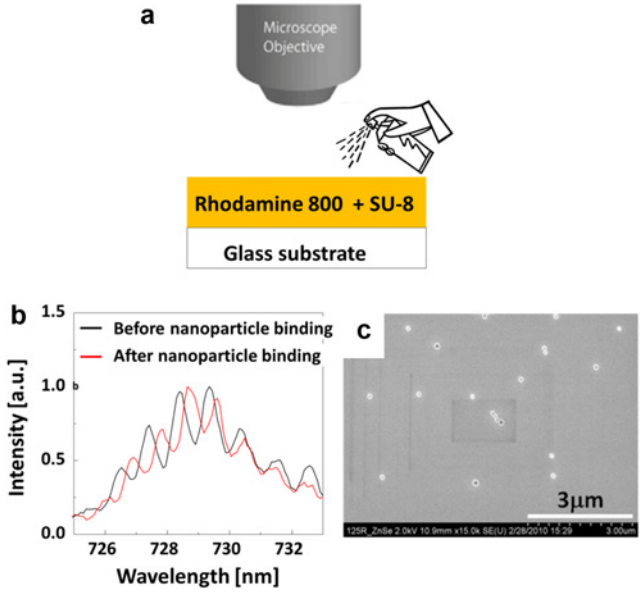

Fig. 4. (a) Illustration of a SEM image of silica nanoparticles on a glass substrate before applying SU8 polymer. (b) The nanoparticle binding causes the spectral shifts of each discrete peak in the emission spectrum. (c) SEM confirmation of ~20 nanoparticles. This figure is reproduced with permission from Ref [91].

Sensitivity and response characteristic upon nanoscale perturbations

The idea that random lasing is sensitive enough to detect single-nanoparticle are also supported by a recent study [91]. Fig. 4 shows the possibility of multimode random lasing to develop a biosensor for detecting a small number of nanoparticles. In this study, to fabricate a simple static nanostructure consisting of nanoparticles and a layer dye, silica nanospheres (diameter = 150 nm) were randomly distributed on a glass substrate and then dye-doped SU-8 prepolymer was spin-coated on the top of the nanosphere layer (thickness = 0.8 μm). Spectral changes in the coherent random lasing emission was measured, by spraying silica nanospheres (diameter = 150 nm) with a nozzle system on the top surface, while keeping all the other conditions unchanged. The study shows clear spectral shifts in each discrete peak induced by the nanoparticle attachment, while the overall spectral shape and the total number of the discrete peaks were almost the same. The SEM image also support the result that there were merely ~20 nanospheres attached

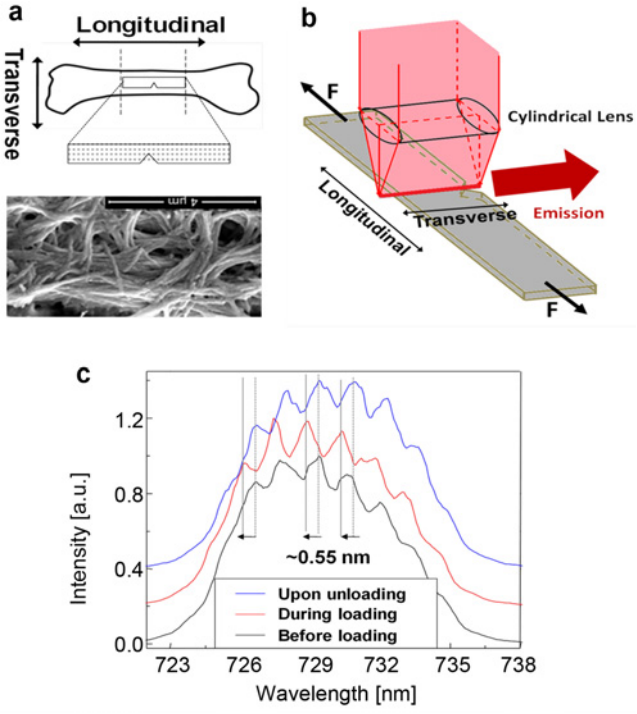

Fig. 5. (a) Bone specimen preparation and representative SEM image of the bone specimen. (b) A narrow strip of the pumping illumination is normally focused onto the bone tissue. A miniaturized tensile testing device is used to introduce tensile force of 9 N (~ 0.03% strain in the transverse orientation). (c) A clear shift of ~ 0.55 nm in the emission peaks under the peak loading. After removal of the loading, the laser peaks restore to the original peak positions. This figure is reproduced with permission from Ref [61].

in the pumping area of ~40 μm^2 (mass per unit area ~ 2.3×10^{-15} g/μm^2 = 3.75×10^{-16} mole/μm^2).

In another coherent random lasing study, bone tissue was used to detect nanoscale prefailure deformation at extremely small strains [61]. As shown in Fig. 5, to induce minimal yet detectable deformation, the tensile force of ~ 9 N was applied on the specimen of a cortical bone specimen along the transverse orientation of the bone structure to maximize light confinement. Under peak loading, the random laser emission peaks were shifted to the left by ~ 0.55 nm. After removal of the loading, they returned to the original spectrum. Because the strain along the longitudinal orientation was ~ 0.17%, using a Poisson's ratio of ~ 0.2 in the cortical bone [92], the strain along the transverse orientation can be estimated to be ~ 0.2 × 0.17% = 0.034% under the experimental conditions. Such subtle deformation would be virtually impossible to detect using conventional methods. The recent studies above support the predictable response of random lasing upon nanoscale perturbations.

Mode alterations upon single-nanoparticle perturbations

A predictable relationship between single-nanoparticle perturbations and emission spectral responses exists even in disordered media [93]. In Fig. 6, random lasing can provide a means to dramatically amplify subtle nanoscale perturbations to readily detectable resonant mode changes. The eigenvalues of the system were calculated to obtain resonant frequencies of the passive system (i.e. quasimodes) and the quality Q factors (= $|\mathrm{Re}(\kappa)/(2\times\mathrm{Im}(\kappa))|$). At an initial stage, the refractive index of the single-nanoparticle was assumed to be $n_{sp} = 1$ and this value gradually increased to describe the perturbation of a single nanoparticle (Fig. 6a). This gradual change was used to evaluate the detection sensitivity to a single nanoparticle and to search possible modes that possess predictable behavior to be implemented for a sensing mechanism. Fig. 6b depicts changes in the quasimodes as n_{sp} is continuously varied from 1 to 1.462. $n_{sp} = 1$ corresponds to the absence of the single-nanoparticle. In Fig. 6b, the open colored circles represent the complex frequencies of the modes, and the edge color of the circles gradually changes from black to orange in the direction of the red arrows as n_{sp} increases from 1 to 1.462. To trace each mode as n_{sp} increases from 1 to 1.462, modes were grouped according to their frequency space trajectory using principal component analysis.[94] As shown in Fig. 6b, multiple modes vary simultaneously in different directions and the spatial distribution of the electric field amplitude is altered significantly (Figs. 6c and 6d) as n_{sp} of the single-nanoparticle increases. The selected quasimodes show linear wavelength shifts as a function of the refractive index (Fig. 6e), which is an important characteristic for sensors. These shifts are inversely proportional to changes in the spatial profile of the quasimode (Fig. 6f). Overall, the single-nanoparticle alterations induce the changes in the multiple modes and can possibly be detected by a shift in any of the multiple modes.

Improving the sensitivity and the signal-to-noise ratio, this multidimensional information from multimodes would provide additional advantages over other conventional biosensing methods that rely on single peaks or single modes to quantify input perturbations. Nanoscale alterations in a disordered medium can induce dramatic changes in the spatial profile of the self-formed optical cavities that can be assessed by

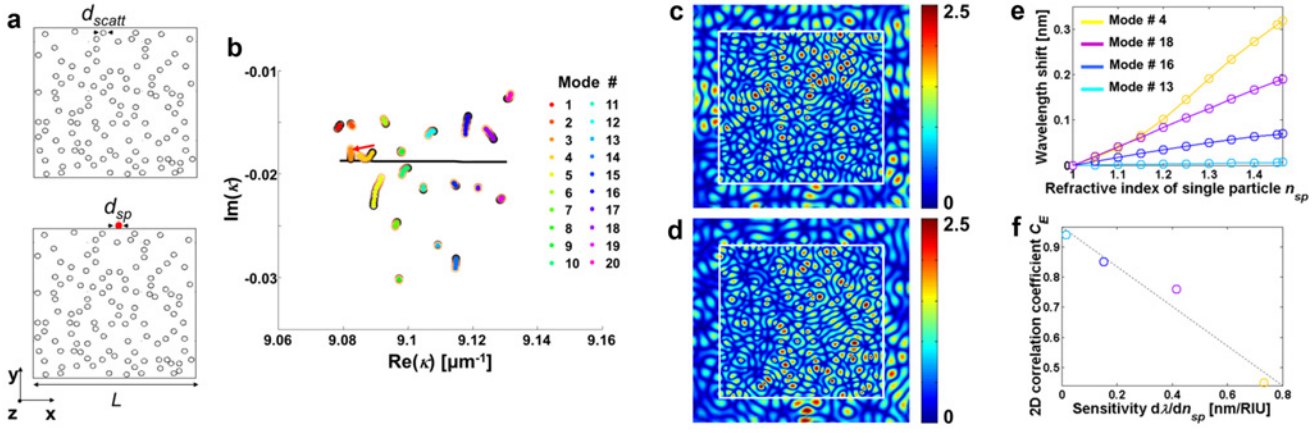

Fig. 6. (a) The scheme of the numerical experiments. The structure consists of 115 randomly distributed nanoparticles. (b) The wavelength shift of representative quasimodes as n of the single nanoparticle (diameter = 200 nm) varies on the top. (c) and (d) show the distribution of the amplitude of the electric field of the mode at around 690 nm (the yellow line in (b)), when n = 1 and 1.46, respectively. The 2D correlation coefficient between (c) and (d) is 0.45, showing a dramatic alteration in the spatial profile of the mode. (e) The selected quasimodes show wavelength shiftsas a function ofthe refractive index of the single nanoparticle on top of structure in a. (f) The sensitivity of eachmode frequency isinversely proportional to 2D correlation coefficientsbetween electric field of before and after the singlenanoparticle introduction.This figure is reproduced with permission from Ref [93].

obtaining the spatial distributions or spectral variations of the random lasing modes. Moreover, such changes in multiple modes (rather than in a single mode) can offer a "fine fishnet" effect to capture any of perturbations in either strongly scattering or weakly scattering systems. If perturbations are extremely small at single-nanoparticle levels, predicable responses could be accurately captured by linear wavelength shifts of the emission spectrum.

Low lasing thresholdusing photon localization

A potential limitation of random laser-based biosensors would be that random lasers require high excitation energy due to the open system, which could potentially hamper practical and widespread applications. Because of the cost of the pump light source, the final system will be too expensive for widespread use in resource-limited settings. In this respect, numerous theoretical and experimental studies have already been conducted by others to understand the dependence of the random lasing threshold, for example,

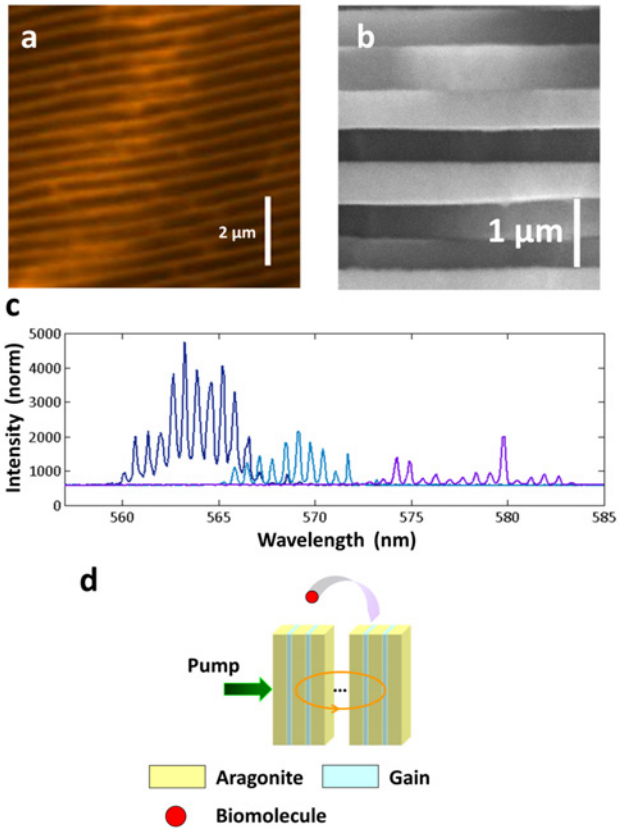

Fig. 7. (a) Confocal fluorescence microscopy image of nacre from an abalone shell infiltrated with Rhodamine 6G (Rh6G) for a multilayered random laser biosensor platform. (b) Scanning electron microscopy image of a brick-mortar structure in nacre. (c) Three representative lasing emission spectra at different locations above the lasing threshold. (d) Schematic diagram of sensing scheme ina multilayered random laser biosensor platform taking advantage of light localization effects.

incorporating disorder in photonic crystal structures [95], photonic bandgaps (edges of stop bands) [96], and 1D photon localization [97]. For low laser threshold, efficient random lasers in nacre (also known as mother-of-pearl) infiltrated with a fluorescent dye (a manuscript is under preparation) have been demonstrated [98]. In this photoluminescence experiment, deproteinized nacre specimens were immersed in a Rhodamine 6G (Rh6G) solution (Fig. 7a) and were optically pumped with a frequency-doubled Nd:YAG laser (pulse duration of 400 ps and wavelength of 532 nm) via an objective lens (5×). The emitted light was collected by a fiber bundle through a lens and coupled to a spectrometer. As shown in Fig. 7b, the layered structures (each thickness ~ 500 nm) drastically lowered the lasing threshold down to 0.6 μJ/pulse. The low lasing threshold and the high energy conversion efficient further allowed multiple discrete emission peaks to be equally spaced in wavelength (Fig. 7c). This study demonstrates that multilayered structures are extremely beneficial to achieve an extremely low lasing threshold and high energy conversion efficiency, leading to well-defined multimode lasing emission. While ordered and closed resonators are commonly thought to be crucial, this biogenic approach using nacre reveals an alternative strategy for designing and fabricating multilayered random laser biosensors (closed to 1D) as shown in Fig. 7d. The recent studies support the usefulness of 1D photon localization structure for significantly improving the random lasing efficiency.

Low lasing threshold using localized surface plasmon resonance (LSPR)

Among other approaches, several recent studies have also demonstrated that the presence of metallic nanoparticles in gain media can significantly reduce the lasing threshold in ASE [62, 99] and coherent random lasers [63, 67, 100, 101]: Relatively large gold nanoparticles (diameter > 100 nm) can improve the lasing efficiency due to the high scattering crosssection [62]. More importantly, the primary mechanism by which small metallic nanoparticles (diameter ~ 1 - 50 nm) dramatically lower the lasing threshold is an enhanced localized electrometric field in the vicinity of the nanoparticles (i.e. LSPR). The enhancement of LSPR-enhanced spontaneous emission can be expressed such that [102-104]

$$E = \frac{\gamma_{exc}}{\gamma_{exc}^{0}}(\lambda_{ex}) \times \frac{q}{q^{0}}(\lambda_{em}) \tag{6}$$

where γ_{ex} is the excitation rate, γ^{0}_{ex} is the corresponding excitation rate in free space, q is the quantum yield of spontaneous emission coupled into LSPR, q^{0} is the corresponding quantum yield in free space, λ_{ex} is the excitation wavelength, and λ_{em} is the emission wavelength of

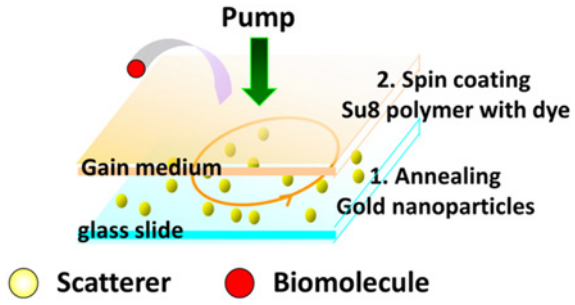

Fig. 8. Schematic diagram of integration of metallic nanoparticles into the 2D random laser biosensor platform to take use of LSPR effects. (b) LSPR-enhanced spontaneous emission in disordered plasmonic systems consisting of Au nanostructures.

fluorophores. Thus, plasmonic bands of metallic nanoparticles are required to overlap with the emission and/or excitation bands of fluorophores [103-106]. It should also be noted that the intrinsic quantum yield of fluorophores sets a limit for the LSPR enhancement. In any fluorophores with a quantum yield of 100%, emission cannot be enhanced anymore. The LSPR-enhanced random lasers reported in the references [63, 67, 100, 101] indicate the quantum yield of spontaneous emission coupled into lasing modes was low, although laser dyes with high quantum efficacies (~ 0.95 for Rh6G) were used. In other words, LSPR can be effective in lowering the lasing threshold and enhancing the conversion efficacy.

Disordered Au nanostructures can allow studying the effects of spectral overlap of plasmonic bands with the excitation/emission wavelength of quantum dots on spontaneous emission enhancement [6]. In this study, disordered Au nanostructures were constructed to obtain a variety of combinations of reflectance intensities at the excitation and emission bands of quantum dots. Colloidal Au nanoparticles on a microscope slide were self-assembled during an annealing procedure. Individual Au clusters in different sizes were formed to generate multiple resonance peaks. The fluorescence enhancement was proportional to the scattering cross-section of metallic nanostructures. The combinations with disorder-driven lasers for biosensors could potentially bring the cost of the system to an acceptable level for widespread and practical applications by eliminating high pump energy. Collectively, this result supports the idea that LSPR will be highly beneficial to lower the random lasing thresholds in conjunction with random lasing biosensor development using higher dimensional structures, as illustrated in Fig. 8.

Functionalization for target biomolecule detection

To implement random lasing in a biosensing system, receptor immobilization or deposition of single molecule should be implemented. The following methods could potentially be used in the random laser biosensors: i) Flowing high charged particle onto the biosensor [31, 107]: In a single-nanoparticle detection study using whispering-gallery-mode (WGM), the charged particle is sprayed onto the metal microtoroid surface. Due to the concentrated WGM field profile, the single particle can be attached at a specific position. ii) Strong biomolecule-receptor pair interaction of biotin and streptavidin [108-113]: Usually, biotinlylated bovine serum albumin (BSA biotin) is used as a target molecules. The optical biosensor platform coated with streptavidin is placed in a microfluidic device (e.g. ibidi channel slides) and then a BSA biotin solution is injected into the slide. The concentration of the BSA biotin solution is gradually varied to determine the binding sensitivity and resolution. iii) Utilization of surface modification for antibody-antigen pair deposition [28, 32, 114-119]: To offer biofunctionality and nonfouling properties for biological and chemical applications, several surface modification methods for polymer materials have been developed. For an antibody-antigen pair (i.e. IgG and anti-IgG), low concentration of human IgG is immobilized on the surface of the structure via crosslinkers. By applying NaOH and HCl, outermost epoxy groups are cleaved and hydroxyl groups are generated. Then, anti-human IgG solution is injected into a bath surrounding the structure. iv) Random interaction by the Brownian motion of particles in liquid [120]: A single particle is suspended in a bath. Unsuccessful attempts of single particle adsorption due to the Brownian motion of a single-nanoparticle on top of the sensor can induce spiky signals.

The methods for receptor immobilization or deposition of single molecules are potentially useful to introduce well-controlled molecular mass density perturbations on the random lasing biosensor and to experimentally test the possibility of single-nanoparticle detection.

CONCLUSION

Our review supports the idea that random lasing in disordered nanostructures could potentially serve as a powerful biosensing mechanism, by showing that random lasing has i) stable, ii) reproducible emission peaks, iii) high sensitivity, and iv) low lasing threshold, and n) can be implemented in biosensing schemes. In addition, moreover, random lasing biosensors can have the following advantages over the conventional biosensors: i) The changes in the multiple modes from perturbations can offer a “fine fishnet” effect to possibly capture any of perturbations. This multidimensional information from the multimodes would provide additional advantages over other conventional biosensing methods that rely on single peaks or single modes to quantify input perturbations. ii) The detection strategy is

straightforward. No precise alignment of the system is required because the output lasing signals can be easily detected in the far field. iii) Simple fabrication can be possible. Random lasing allows defect in fabrication that would be advantageous over other small and complicated photonic structured sensors. Overall, these unique and intriguing characteristics of coherent random lasers could potentially be transformed into a wide range of multimodal sensing platforms (e.g. spectroscopy scheme [61, 71, 91], multiplexed scheme [121, 122], or imaging scheme) for biological, chemical, and environmental applications.

ACKNOWLEDGEMENTS

This work was supported in part by the grants from Abbott Laboratories and NIH (R21 ES020965).

CONFLICT OF INTEREST STATEMENTS

Choi SH declares that he has no conflict of interest in relation to the work in this article. Kim YL declares that he has no conflict of interest in relation to the work in this article.

REFERENCES

[1] Sako Y, Minoghchi S, Yanagida T. Single-molecule imaging of EGFR signalling on the surface of living cells. Nat Cell Biol. 2000; 2(3):168-72.
[2] Jablonski AE, Humphries WH, Payne CK. Pyrenebutyrate-mediated delivery of quantum dots across the plasma membrane of living cells. J Phys Chem B. 2009; 113(2):405-8.
[3] Lipman EA, Schuler B, Bakajin O, A. EW. Single-molecule measurement of protein folding kinetics. Science. 2003; 301(5637):1233-5.
[4] Lang MJ, Fordyce PM, Engh AM, Neuman KC, Block SM. Simultaneous, coincident optical trapping and single-molecule fluorescence. Nat Methods. 2004; 1(2):133-39.
[5] Lavrinenko AV, Wohlleben W, Leyrer RJ. Influence of imperfections on the photonic insulating and guiding properties of finite Si-inverted opal crystals. Opt Express. 2009; 17(2):747-60.
[6] Choi SH, Kwak B, Han B, Kim YL. Competition between excitation and emission enhancements of quantum dots on disordered plasmonic nanostructures. Opt Express. 2012; 20(15):16785-93.
[7] Huang B, Wu H, Bhaya D, Grossman A, Granier S, Kobilka BK, Zare RN. Counting low-copy number proteins in a single cell. Science. 2007; 315(5808):81-4.
[8] Elf J, Li GW, Xie XS. Probing transcription factor dynamics at the single-molecule level in a living cell. Science. 2007; 316(5828):1191-4.
[9] Moore BD, Stevenson L, Watt A, Flitsch S, Turner NJ, Cassidy C, Graham D. Rapid and ultra-sensitive determination of enzyme activities using surface-enhanced resonance Raman scattering. Nat Biotechnol. 2004; 22(9):1133-8.
[10] Kulkarni RP, Castelino K, Majumdar A, Fraser SE. Intracellular transport dynamics of endosomes containing DNA polyplexes along the microtubule network. Biophys J. 2006; 90(5):L42-4.
[11] Funatsu T, Harada Y, Tokunaga M, Saito K, Yanagida T. Imaging of single fluorescent molecules and individual ATP turnovers by single myosin molecules in aqueous solution. Nature. 1995; 374(6522):555-9.
[12] Myong S, Rasnik I, Joo C, Lohman TM, Ha T. Repetitive shuttling of a motor protein on DNA. Nature. 2005; 437(7063):1321-5.
[13] Cao YWC, R. J, A. MC. Nanoparticles with raman spectroscopic fingerprints for dna and rna detection. Science. 2002; 297(5586):1536-40.
[14] Hughes RC, Ricco AJ, Butler MA, Martin SJ. Chemical microsensors. Science. 1991; 254(5028):74-80.
[15] Copper MA. Optical biosensors in drug discovery. Nat Rev Drug Discov. 2002; 1(7):515-28.
[16] Choi SH, Kim YL, Byun KM. Graphene-on-silver substrates for sensitive surface plasmon resonance imaging biosensors. Opt Express. 2011; 19(2):458-66.
[17] Choi SH, Byun KM. Investigation on an application of silver substrates for a sensitive surface plasmon resonance imaging detection. J Optl Soc of Am A. 2010; 27(10):2229-36.
[18] Choi SH, Kim SJ, Byun KM. Characteristics of light emission from surface plasmons based on rectangular silver gratings. Opt Commun. 2010; 283(14):2961-6.
[19] Choi SH, Kim SJ, Byun KM. Design study for transmission improvement of resonant surface plasmons using dielectric diffraction gratings. Appl Opt. 2009; 48(15):2924-31.
[20] Piehler J, A. B, G. G. Affinity detection of low molecular weight analyte. Anal Chem. 1996; 68(1):139-43.
[21] Cross GH, Reeves A, Brand S, Swann MJ, Peel LL, Freeman NJ, Lu JR. The metrics of surface adsorbed small molecules on the Young's fringe dual-slab waveguide interferometer. J Phys D Appl Phys. 2004; 37(1):74-80.
[22] Choi CJ, Block ID, Bole B, Dralle D, Cunningham BT. Label-free photonic crystal biosensor integrated microfluidic chip for determination of kinetic reaction rate constants. IEEE Sens J. 2009; 9(12):1697-704.
[23] Cunningham BT, Li P, Schulz S, Lin B, Baird C, Gerstenmaier J, Genick C, Wang F, Fine E, Laing L. Label-free assays on the bind system. J Biomol Screen. 2004; 9(6):481-90.
[24] Nam JM, Thaxton CS, Mirkin CA. Nanoparticle-based bio-bar codes for the ultrasensitive detection of proteins. Science. 2003; 301(5641):1884-6.
[25] Zhong Z, Wang D, Cui Y, Bockrath MW, Lieber CM. Nanowire crossbar arrays as address decoders for integrated nanosystems. Science. 2003; 302: 302(5649):1377-9.
[26] Burg TP, Godin M, Knudsen SM, Shen W, Carlson G, Foster JS, Babcock K, Manalis SR. Weighing of biomolecules, single cells and single nanoparticles in fluid. Nature. 2007; 446(7139):1066-9.
[27] Yeo WS, Min DH, Hsieh RW, Greene GL, Mrksich M. Label-free detection of protein-protein interactions on biochips. Angew Chem Int Edit. 2005; 44(34):5480-3.
[28] Armani AM, Kulkarni RP, Fraser SE, Flagan RC, Vahala KJ. Label-free, single-molecule detection with optical microcavities. Science. 2007; 317(5839):783-7.
[29] Vollmer F, Arnold S. Whispering-gallery-mode biosensing: label-free detection down to single molecules. Nat Methods. 2008; 5(7):591-6.
[30] Harker A, Mehrabani S, Armani AM. Ultraviolet light detection using an optical microcavity. Opt Lett. 2013; 38(17):3422-5.

[31] Zhu J, Ozdemir SK, Xiao YF, Li L, He L, Chen DR, Yang L. On-chip single nanoparticle detection and sizing by mode splitting in an ultrahigh-Q microresonator. Nat Photonics. 2010; 4(1):46-9.
[32] Dominguez-Juarez JL, Kozyreff G, Martorell J. Whispering gallery microresonators for second harmonic light generation from a low number of small molecules. Nat Commun. 2011; doi:10.1038/ncomms1253.
[33] Koenderink AF, Lagendijk A, Vos WL. Optical extinction due to intrinsic structural variations of photonic crystals. Phys Rev B. 2005; doi:10.1103/PhysRevB.72.153102.
[34] Toninelli C, Vekris E, Ozin GA, John S, Wiersma DS. Exceptional reduction of the diffusion constant in partially disordered photonic crystals. Phys Rev Lett. 2008; doi:10.1103/PhysRevLett.101.123901.
[35] Woldering LA, Mosk AP, Tjerkstra RW, Vos WL. The influence of fabrication deviations on the photonic band gap of three-dimensional inverse woodpile nanostructures. J Appl Phys. 2009; doi:10.1063/1.3103777.
[36] Lavrinenko AV, Wohlleben W, Leyrer RJ. Influence of imperfections on the photonic insulating and guiding properties of finite Si-inverted opal crystals. Opt Express. 2009; 17(2):747-60.
[37] Wiersma DS. Disordered photonics. Nat Photonics 2013; 7(3):188-96.
[38] Cao H. Review on latest developments in random lasers with coherent feedback. J Phys A-Math Gen. 2005; 38(49):10497-535.
[39] Noginov M. Solid-State Random Lasers. 1st ed. Berlin: Springer; 2005.
[40] Wiersma DS. The physics and applications of random lasers. Nat Phys. 2008; 4(5):359-67.
[41] Nishijima Y, Ueno K, Juodkazis S, Mizeikis V, Fujiwara H, Sasaki K, Misawa H. Lasing with well-defined cavity modes in dye-infiltrated silica inverse opals. Opt Express. 2009; 17(4):2976-83.
[42] Wiersma DS, van Albada MP, van Tiggelen BA, Lagendijk A. Experimental evidence for recurrent multiple-scattering events of light in disordered media. Phys Rev Lett. 1995; 74(21):4193-6.
[43] Polson RC, Chipouline A, Vardeny ZV. Random lasing in pi-conjugated films and infiltrated opals. Adv Mater. 2001; 13(10):760-4.
[44] Kim YL, Turzhitsky VM, Liu Y, Roy HK, Wali RK, Subramanian H, Pradhan P, Backman V. Low-coherence enhanced backscattering: Review of principles and applications for colon cancer screening. J Biomed Opt. 2006; doi:10.1117/1.2236292.
[45] Wang W, Wu N, Tian Y, Wang X, Niezrecki C, Chen J. Optical pressure/acoustic sensor with precise Fabry-Perot cavity length control using angle polished fiber. Opt Express. 2009; 17(19):16613-8.
[46] Hill GC, Melamud R, Declercq FE, Davenport AA, Chan IH, Hartwell PG, Pruitt BL. SU-8 mems fabry-perot pressure sensor. Sensors Actuat a-Phys. 2007; 138(1):52-62.
[47] Cunningham BT. Label-free optical biosensors: An introduction. New York: Cambridge University Press; 2009.
[48] Kringlebotn J, Archambault J, Reekie L, Payne D. Er3+yb3+ codoped fiber distributed-feedback laser. Opt Lett. 1994; 19(24):2101-3.
[49] Koo KP, Kersey AD. bragg grating-based laser sensors systems with interferometric interrogation and wavelength-division multiplexing. J Lightwave Technol. 1995; 13(7):1243-9.
[50] Mujumdar S, Ricci M, Torre R, Wiersma DS. Amplified extended modes in random lasers. Phys Rev Lett. 2004; doi:10.1103/PhysRevLett.93.053903.
[51] Mujumdar S, Türck V, Torre R, Wiersma DS. Chaotic behavior of a random laser with static disorder. Phys Rev A. 2007; doi:10.1103/PhysRevA.76.033807.
[52] Polson RC, Vardeny ZV. Random lasing in human tissues. Appl Phys Lett. 2004; 85(7):1289-91.
[53] Polson RC, Vardeny ZV. Organic random lasers in the weak-scattering regime. Phys Rev B. 2005; doi:10.1103/PhysRevB.71.045205.
[54] Tulek A, Polson RC, Vardeny ZV. Naturally occurring resonators in random lasing of •š-conjugated polymer films. Nat Phys. 2010; 6(4):303-10.
[55] Wiersma DS, Cavalieri S. Light emission: a temperature-tunable random laser. Nature. 2001; 414(6865):708-9.
[56] Rose A, Zhu Z, Madigan CF, Swager TM, Bulovиæ V. Sensitivity gains in chemosensing by lasing action in organic polymers. Nature. 2005; 434(7035):876-9.
[57] Deng C, He Q, He C, Shi L, Cheng J, Lin T. Conjugated polymer-titania nanoparticle hybrid films: random lasing action and ultrasensitive detection of explosive vapors. J Phys Chem B. 2010; 114(13):4725-30.
[58] Letokhov VS. Generation of light by a scattering medium with negative resonance absorption. Sov J Phys. 1968; 26(4):835-40.
[59] Lawandy NM, Balachandran RM, Gomes ASL, Sauvain E. Laser action in strongly scattering media. Nature. 1994; 368(6470):436-8.
[60] Pradhan P, Kumar N. Localization of light in coherently amplifying random-media. Phys Rev B. 1994; 50(13):9644-7.
[61] Song Q, Xu Z, Choi SH, Sun X, Xiao S, Akkus O, Kim YL. Detection of nanoscale structural changes in bone using random lasers. Biomed Opt Express. 2010; 1(5):1401-7.
[62] Popov O, Zilbershtein A, Davidov D. Random lasing from dye-gold nanoparticles in polymer films: enhanced gain at the surface-plasmon-resonance wavelength. Appl Phys Lett. 2006; doi:10.1063/1.2364857.
[63] Dominguez CT, Maltez RL, dos Reis RMS, de Melo LSA, de Araújo CB, Gomes ASL. Dependence of random laser emission on silver nanoparticle density in PMMA films containing rhodamine 6G. J Opt Soc Am B. 2011; 28(5):1118-23.
[64] Cao H, Zhao YG, Ho ST, Seelig EW, Wang QH, Chang RPH. Random laser action in semiconductor powder. Phys Rev Lett. 1999; 82(11):2278-81.
[65] Vanneste C, Sebbah P, Cao H. Lasing with resonant feedback in weakly scattering random systems. Phys Rev Lett, 2007. doi:10.1103/PhysRevLett.98.143902.
[66] Muskens OL, Diedenhofen SL, Kaas BC, Algra RE, Bakkers EP, Rivas JG, Lagendijk A. Large photonic strength of highly tunable resonant nanowire materials. Nano Lett. 2009; 9(3):930-4.
[67] Meng X, Fujita K, Murai S, Matoba T, Tanaka K. Plasmonically controlled lasing resonance with metallic-dielectric core-shell nanoparticles. Nano Lett. 2011; 11(3):1374-8.
[68] Siddique M, Yang L, Wang QZ, Alfano RR. Mirrorless laser action from optically pumped dye-treated animal-tissues. Opt Commun. 1995; 117(5-6):475-9.
[69] Wang L, Liu D, He N, Jacques SL, Thomsen SL. Biological laser action. Appl Opt. 1996; 35(10):1775-9.
[70] Polson RC, Vardeny ZV. Random lasing in human tissues. Appl Phys Lett. 2004; 85(7):1289-91.
[71] Song Q, Xiao S, Xu Z, Liu J, Sun X, Drachev V, Shalaev VM, Akkus O, Kim YL. Random lasing in bone tissue. Opt Lett. 2010; 35(9):1425-7.
[72] Gather MC, Yun SH. Single-cell biological lasers. Nat Photonics. 2011; 5(7):406-10.
[73] Jiang X, Soukoulis CM. Localized random lasing modes and a path for observing localization. Phys Rev E. 2002; doi:10.1103/PhysRevE.65.025601.
[74] Jiang X, Soukoulis CM. Transmission and reflection studies of periodic and random systems with gain. Phys Rev B. 1999;

59(9):6159-66.
[75] Choi K, Kim H, Lim Y, Kim S, Lee B. Analysis design and visualization of multiple surface plasmon resonance excitation using angular spectrum decomposition for a gaussian input beam. Opt Express. 2005; 13(22):8866-74.
[76] Hecht E. Optics. 4th ed. Seoul: Addison Wesley Longman; 2002.
[77] Vanneste C, Sebbah P. Selective excitation of localized modes in active random media. Phys Riv Lett. 2001; doi:10.1103/PhysRevLett.87.183903.
[78] Andreasen J, Asatryan AA, Botten LC, Byrne MA, Cao H, Ge L, Labonté L, Sebbah P, Stone AD, Türeci HE, Vanneste C. Modes of random lasers. Adv Opt Photonics. 2011; 3(1):88-127.
[79] Wu X, Fang W, Yamilov A, Chabanov AA, Asatryan AA, Botten LC, Cao H. Random lasing in weakly scattering systems. Phys Rev A. 2006; doi:10.1103/PhysRevA.74.053812.
[80] Ge L, Tandy RJ, Stone AD, Türeci HE. Quantitative verification of ab initio self-consistent laser theory. Opt Express. 2008; 16(21):16895-902.
[81] Wu XH, Yamilov A, Noh H, Cao H, Seelig EW, Chang RP. Random lasing in closely packed resonant scatterers. J Opt Soc Am B. 2004; 21(1):159-67.
[82] Jin J. The finite element method in electromagnetics. 2nd ed. New York: John Wiley & Sons; 1993.
[83] Becker EB, Carrey GF, Oden JT. Finite elements: An introduction. NewJersey: Prentice Hall; 1981.
[84] Wu XH, Cao H. Statistics of random lasing modes in weakly scattering systems. Opt Lett. 2007; 32(21):3089-91.
[85] Wu X, Cao H. Statistical studies of random-lasing modes and amplified spontaneous-emission spikes in weakly scattering systems. Phys Rev A. 2008; doi:10.1103/PhysRevA.77.013832.
[86] Tseng S, Kim Y, Taflove A, Maitland D, Backman V, Walsh J. Simulation of enhanced backscattering of light by numerically solving Maxwell's equations without heuristic approximations. Opt Express. 2005; 13(10):3666-72.
[87] Fallert J, Dietz RJ, Sartor J, Schneider D, Klingshirn C, Kalt H. Co-existence of strongly and weakly localized random laser modes. Nat Photonics. 2009; 3(5):279-82.
[88] Frolov SV, Vardeny ZV, Yoshino K, Zakhidov A, Baughman RH. Stimulated emission in high-gain organic media. Phys Rev B. 1999; doi:10.1103/PhysRevB.59.R5284.
[89] Van der Molen KL, Tjerkstra RW, Mosk AP, Lagendijk A. Spatial extent of random laser modes. Phys Rev Lett. 2007; doi:10.1103/PhysRevLett.98.143901.
[90] Sebbah P, Vanneste C. Random laser in the localized regime. Phys Rev B. 2002; doi:10.1103/PhysRevB.66.144202.
[91] Song Q, Xiao S, Xu Z, Shalaev VM, Kim YL. Random laser spectroscopy for nanoscale perturbation sensing. Opt Lett. 2010; 35(15):2624-6.
[92] Shahar R, Zaslansky P, Barak M, Friesem AA, Currey JD, Weiner S. Anisotropic poisson's ratio and compression modulus of cortical bone determined by speckle interferometry. J Biomech. 2007; 40(2):252-64.
[93] Choi S, Kim YL. Random lasing mode alterations by single-nanoparticle perturbations. Appl Phys Lett. 2012; doi:10.1063/1.3675885.
[94] Jolliffe IT. Principal Component Analysis. 2nd ed. Springer-Verlag; 1986.
[95] Yamilov A, Cao H. Highest-quality modes in disordered photonic crystals. Phys Rev A. 2004; doi:10.1103/PhysRevA.69.031803.
[96] Kopp VI, Fan B, Vithana HK, Genack AZ. Low-threshold lasing at the edge of a photonic stop band in cholesteric liquid crystals. Opt Lett. 1998; 23(21):1707-9.
[97] Milner V, Genack AZ. Photon localization laser: low-threshold lasing in a random amplifying layered medium via wave localization. Phys Rev Lett. 2005; doi:10.1103/PhysRevLett.94.073901.
[98] Choi SH, Kim YL. Hybridized/coupled multiple resonances in nacre. Phys Rev B. 2014; doi:10.1103/PhysRevB.89.035115.
[99] Dice GD, Mujumdar S, Elezzabi AY. Plasmonically enhanced diffusive and subdiffusive metal nanoparticle-dye random laser. Appl Phys Lett. 2005; doi:10.1063/1.1894590.
[100] Meng X, Fujita K, Zong Y, Murai S, Tanaka K. Random lasers with coherent feedback from highly transparent polymer films embedded with silver nanoparticles. Appl Phys Lett. 2008; doi:10.1063/1.2912527.
[101] Meng X, Fujita K, Murai S, Tanaka K. Coherent random lasers in weakly scattering polymer films containing silver nanoparticles. Phys Rev A. 2009; doi:10.1103/PhysRevA.79.053817.
[102] Anger P, Bharadwaj P, Novotny L. Enhancement and quenching of single-molecule fluorescence. Phys Rev Lett. 2006; doi:10.1103/PhysRevLett.96.113002.
[103] Bharadwaj P, Novotny L. Spectral dependence of single molecule fluorescence enhancement. Opt Express. 2007; 15(21):14266-74.
[104] Choi SH, Kwak B, Han B, Kim YL. Competition between excitation and emission enhancements of quantum dots on disordered plasmonic nanostructures. Opt Express. 2012; 20(15):16785-93.
[105] Chen Y, Munechika K, Ginger DS. Dependence of fluorescence intensity on the spectral overlap between fluorophores and plasmon resonant single silver nanoparticles. Nano Lett. 2007; 7(3):690-6.
[106] Zhang Y, Dragan A, Geddes CD. Wavelength dependence of metal-enhanced fluorescence. J Phys Chem C. 2009; 113(28):12095-100.
[107] Arnold S, Keng D, Shopova SI, Holler S, Zurawsky W, Vollmer F. Whispering gallery mode carousel – a photonic mechanism for enhanced nanoparticle detection in biosensing. Opt Express. 2009; 17(8):6230-8.
[108] Lin VS, Motesharei K, Dancil KP, Sailor MJ, Ghadiri MR. A porous silicon-based optical interferometric biosensor. Science. 1997; 278(5339):840-3.
[109] Morgan H, Taylor DM. A surface plasmon resonance immunosensor based on the streptavidin-biotin complex. Biosens Bioekctron. 1992; 7(6):405-10.
[110] Abel AP, Weller MG, Duveneck GL, Ehrat M, Widmer HM. Fiber-optic evanescent wave biosensor for the detection of oligonucleotides. Anal Chem. 1996; 68(17):2905-12.
[111] Rehák M, Šnejdárková M, Otto M. Application of biotin-streptavidin technology in developing a xanthine biosensor based on a self-assembled phospholipid membrane. Biosens Bioelectron. 1994; 9(4):337-41.
[112] Kim DS, Park HJ, Park JE, Shin JK, Kang SW, Seo HI, Lim G. Mosfet-type biosensor for detection of streptavidin–biotin protein complexes. Sensors Mater. 2005; 17(5):259-68.
[113] Jung YK, Park HG, Kim JM. Polydiacetylene (PDA)-based colorimetric detection of biotin–streptavidin interactions. Biosens Bioelectron. 2006; 21(8):1536-44.
[114] Tao SL, Popat KC, Norman JJ, Desai TA. Surface modification of SU-8 for enhanced biofunctionality and nonfouling properties. Langmuir. 2008; 24(6):2631-6.
[115] Sadana A, Ram AB. Fractal analysis of antigen-antibody binding kinetics: biosensor applications. Blotechnol Progr. 1994; 10(3):291-8.
[116] Olkhov RV, Shaw AM. Label-free antibody–antigen binding detection by optical sensor array based on surface-synthesized gold nanoparticles. Biosens Bioelectron. 2008; 23(8):1298-302.
[117] Nogues C, Leh H, Langendorf CG, Law RH, Buckle AM, Buckle M. Characterisation of peptide microarrays for studying antibody-antigen binding using surface plasmon resonance imagery. PLoS One. 2010; doi:10.1371/journal.pone.0012152.

[118] Chen Z, Sadana A. An analysis of antigen-antibody binding kinetics for biosensor applications utilized as a model system: influence of non-specific binding. Biophys Chem. 1996; 57(2-3):177-87.
[119] Sutaria M, Sadana A. Dual-fractal analysis for antigen-antibody binding kinetics for biosensor applications. Biotechnol Progr. 1997; 13(4):464-73.
[120] Vollmer F, Arnold S, Keng D. Single virus detection from the reactive shift of a whispering-gallery mode. P Natl Acad Sci USA. 2008; 105(52):20701-4.
[121] Polson RC, Vardeny ZV. Spatially mapping random lasing cavities. Opt Lett. 2010; 35(16):2801-3.
[122] Cao H, Ling Y, Xu JY, Burin AL. Probing localized states with spectrally resolved speckle techniques. Phys Rev E. 2002; doi:10.1103/PhysRevE.66.025601.